

# Gulf of Mexico Hydrate Mapping and Interpretation Analysis

Project Area 3 Report  
Alexey Portnov and Ann Cook

June 30, 2020

This report satisfies Mapping and Prospect Identification within Project Area 3 for BOEM award Gulf of Mexico Gas Hydrate Mapping and Interpretation Analysis, which is Deliverable/Milestone #4 (Table 1).

## Table of Contents

1.	Study area and data.....	2
2.	Using RMS for mapping bottom simulating reflections and paleo-channels .....	5
3.	Results in Project Area 3.....	11
	3.1 Paleo-channels.....	11
	3.2 Bottom simulating reflections .....	11
4.	Results in Zones 1-5.....	14
	4.1 Zone 1 .....	14
	4.2 Zone 2 .....	17
	4.3 Zones 3-5 .....	17
5.	Gas resource estimates .....	24
6.	Conclusions.....	24
7.	References.....	24

Table 1. List of required deliverables and figures.

	Deliverable	Figure #
1	A map showing the distribution of shallow turbidite channel levee systems and shallow salt bodies	6, 9
2	A map showing the depth to the BSR and the spatial distribution of BSRs	5, 7, 8, 9
3	Regional seismic cross sections showing the base of gas hydrate stability and the relationship of prospective reservoir intervals to channel levee systems, faults, salt, and other geologic features	10, 12, 13, 14, 15, 16, 17
4	Subsurface geologic/geophysical maps at the base of gas hydrate stability as determined through mapping, modeling and the integration of well log data	10, 12, 14, 15, 16, 17
5	Subsurface geologic maps of one or more seismic reflectors within the gas hydrate stability zone (or that cross the gas hydrate stability zone) that have a high probability of containing coarse-grained sand based on well log analysis and the nature of the seismic reflector. Maps will include both structural and amplitude renderings.	14, 16 (structure maps)
6	Interpreted seismic lines that illustrate geologic features related to the prospective reservoirs including BSRs, faults, base of gas hydrate stability, and zones of interest.	10, 11, 12, 13, 14, 15, 16, 17
7	If wells occur in the vicinity of the prospect, annotated well-logs at each gas hydrate prospect showing the thickness of hydrates within the stability zone, interpreted base of gas hydrate stability, and the presence of free gas beneath the gas hydrate stability zone.	11, 13

## 1. Study area and data

Project Area 3 is located in the northeastern Gulf of Mexico at the western margin of the Mississippi Canyon in ~250-1500 meters of water (Figure 1a, b). Project Area 3 extends from the continental shelf segment of the Canyon to its slope segment at the head of the uppermost Mississippi fan lobe. In the northeast, Area 3 is characterized by canyon re-entrants and cross-slope ridges with gentle slopes (0.5-2.7 deg), multiple seafloor escarpments and residual knolls indicating active mass wasting at the canyon western sidewall (Figure 1b). All these features and their formation mechanisms have been previously discussed in literature (Goodwin & Prior, 1989). In the northwest, there is a steep drop in the seafloor topography in places reaching ~75 m (Figure 1b). Laterally it extends for several tens of kilometers and resembles a head scarp of a large submarine slide, yet seismic data shows that this bathymetric feature is generated by a high-displacement fault rooting at the top of salt (~2.5 sec TWT). Northern part of the study area is characterized by a complex stratigraphic sequence resulted from Mississippi Canyon incision and development, slope processes and cyclic prodeltaic sedimentation (Goodwin & Prior, 1989). Zones 1 and 2 are located at the margin of the canyon fill, which onlaps onto the underlying bedded shelf deposits (Figure 2). Gas hydrate may occur here in shelf deposits as well as in mass transport deposits and prodeltaic canyon sediments delivered from the Mississippi river delta, especially in Zone 1 where a BSR at the feather edge of GHSZ was observed. However, given a relatively young age of the Mississippi Canyon (<30 ka) (Goodwin & Prior, 1989), cyclic sedimentation and significant eustatic sea level changes, the processes of gas hydrate formation and recycling in Zone 1 are likely particularly complex and require additional study, which is beyond the scope of this report. In the central part of the study area bathymetry is relatively smooth with several large doming features and ridges above buried salt diapirs as well as local (0.5-3 km wide) seafloor mounds, likely mud volcanoes or pingos (Figure 1b). One of these mounds in Block MC 798 (Zone 2) was reported to contain gas hydrate (Geresi et al., 2002; Neurauter & Bryant, 1989). In the deeper part of Project Area 3 (Zones 3-5), gas hydrates are expected in salt roof reservoirs characterized by clustered BSRs, which are common for the Gulf of Mexico. However, given poor seismic data quality and absence of wells, hydrate accumulations in Zones 3-5 are low-confidence.

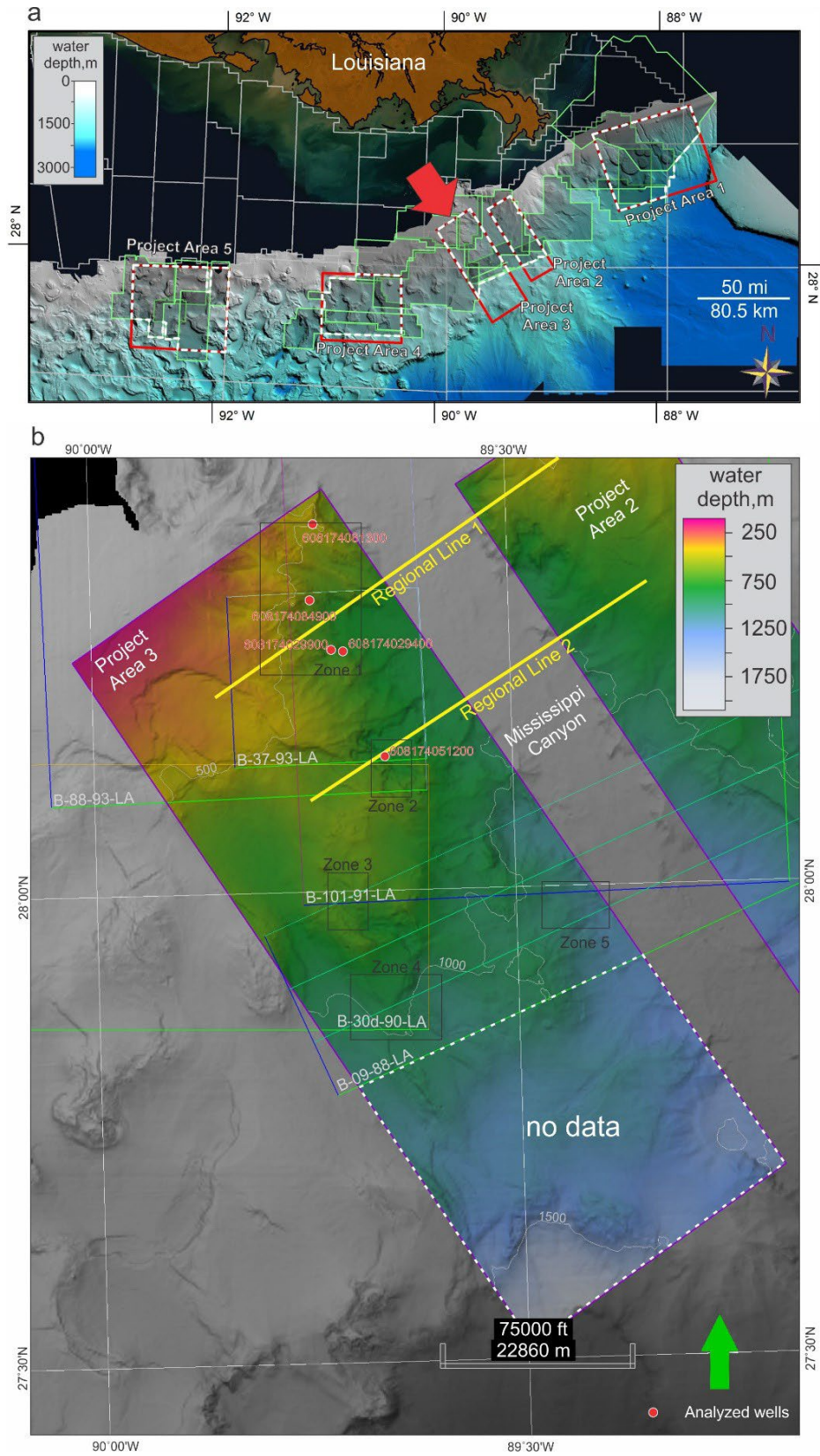


Figure 1 a) A bathymetry map of the northern Gulf of Mexico and five Project Areas. The location of Project Area 3 is defined with the red arrow. b) The bathymetry map and location of five 3D seismic surveys selected for interpretation based on the data quality assessment. See Table 2 for details. Five analyzed wells are marked with red circles and labeled. Zones of interest are marked with black boxes and labeled. No seismic data are available in the dashed white area.



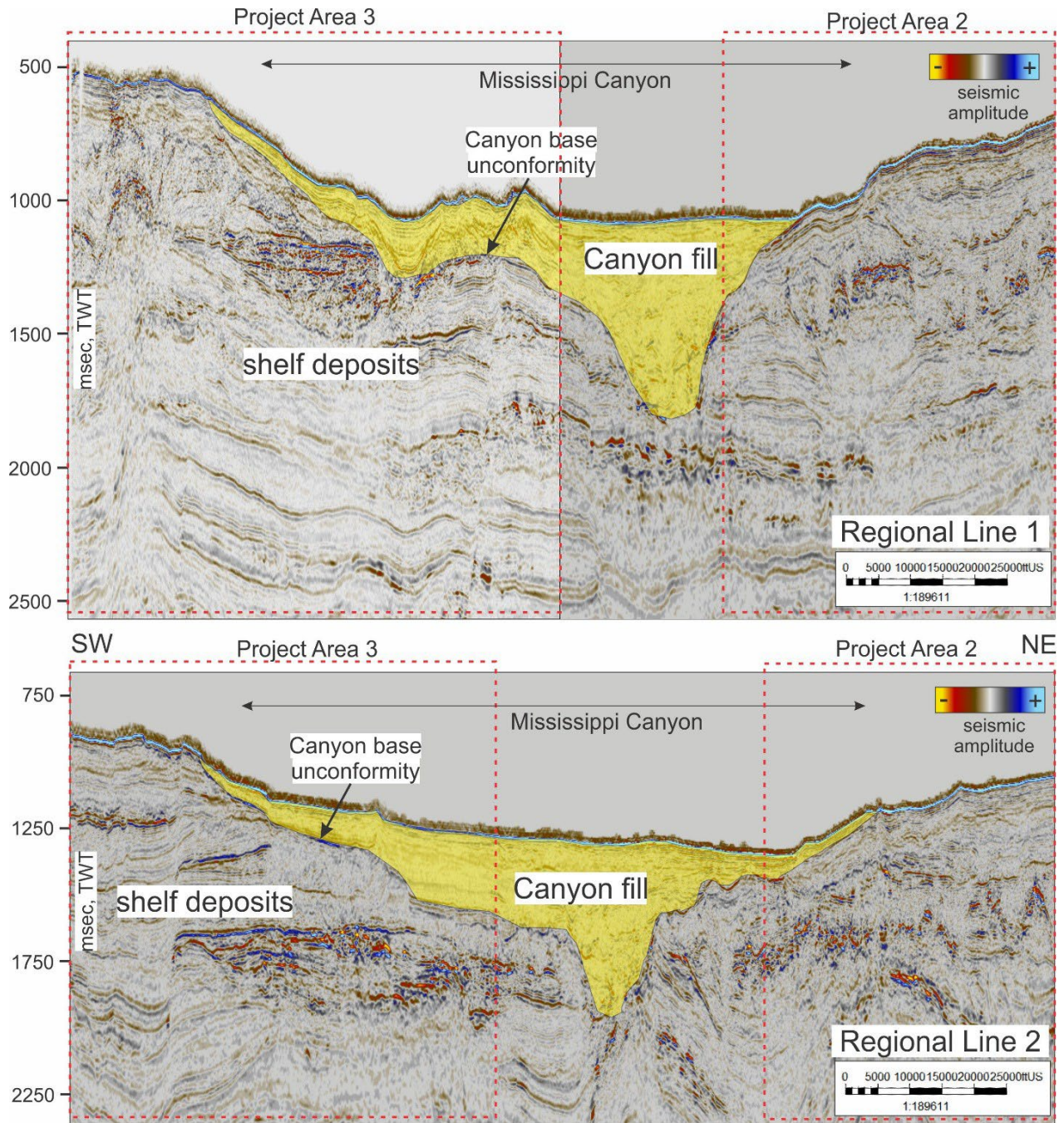


Figure 2. Regional Line 1 (top) and regional Line 2 (bottom) across the Mississippi Canyon showing canyon fill extent in Project Area 3. Locations of both lines are indicated in Figure 1b.

Within Project Area 3, five seismic surveys were exported from the NAMSS database for data quality assessment (Figure 1b, Table 2). The total area of Project Area 3 is 3471 km<sup>2</sup> of which ~2257 km<sup>2</sup> (65%) had 3D seismic data coverage. Based on spatial coverage and data quality, we selected all five surveys to perform further data analyses and interpretation.

Table 2. Details on the 3D seismic surveys uploaded for initial data quality analyses within Project Area 3. Yellow color marks surveys selected for further data interpretation.

Survey number	Survey name/BOEM identifier	Project Area #	Year	Number of 3D volumes	Area of seismic survey (km <sup>2</sup> )	Frequency range (Hz)	Bin size (m)	Projection	Comments
1	B-37-93-LA/L93-037	3	1993	2	484	5-70	25x12.5	16N NAD27, feet	
2	B-88-93-LA/L93-088	3	1993	3	1826	5-77	25x12.5	16N NAD27, feet	
3	B-101-91-LA/L91-101	2 and 3	1991	7	3612	5-90	26x26	16N NAD27, feet	
4	B-30d-90-LA/L90-030	3	1990	3	2246	5-72	25x26	15N NAD27, feet	
5	B-09-88-LA/L88-056	2 and 3	1988	4	1951	10-60	30x30	16N NAD27, feet	Survey is not merged due to problem with coordinates (3 separate volumes)

## 2. Using RMS for mapping bottom simulating reflections, paleo-channels and landslides

To identify the bottom simulating reflections (BSR) in Project Area 3, regional root-mean-square (RMS) amplitude calculations were performed independently within all 3D seismic surveys (Figure 3). According to the workflow explained in Project Area 1 report, we subdivided the study area into three domains based on the water depth (600-800 ms, 800-1300 ms and >1300 ms TWT). Within each domain we applied appropriate parameters for surface and volume attribute analyses to scan the target depth intervals where BSR can exist (please refer to Chapter 2 of the Project Area 1 report for more technical details).

We generated two separate regional RMS maps: the major one, built for mapping the BSR distribution (Figures 3, 5), and the secondary map, primarily targeting buried channels and landslides (Figures 4, 6, 7). Construction of the secondary RMS map did not follow any strict protocol and used locally relevant reference horizons and time windows to better visualize targeted seafloor features. Later, pieces of the maps derived from various seismic volumes were stitched together. Secondary RMS map better shows local channelizing and especially the mass wasting areas in the southern part of Project Area 3 (Figure 7). Due to complex stratigraphy and poor data quality, channel mapping was particularly problematic and in many places was performed manually based on line-by-line interpretation. In the central and southern part of the area, widespread landslide features made channel and BSR identification especially problematic.



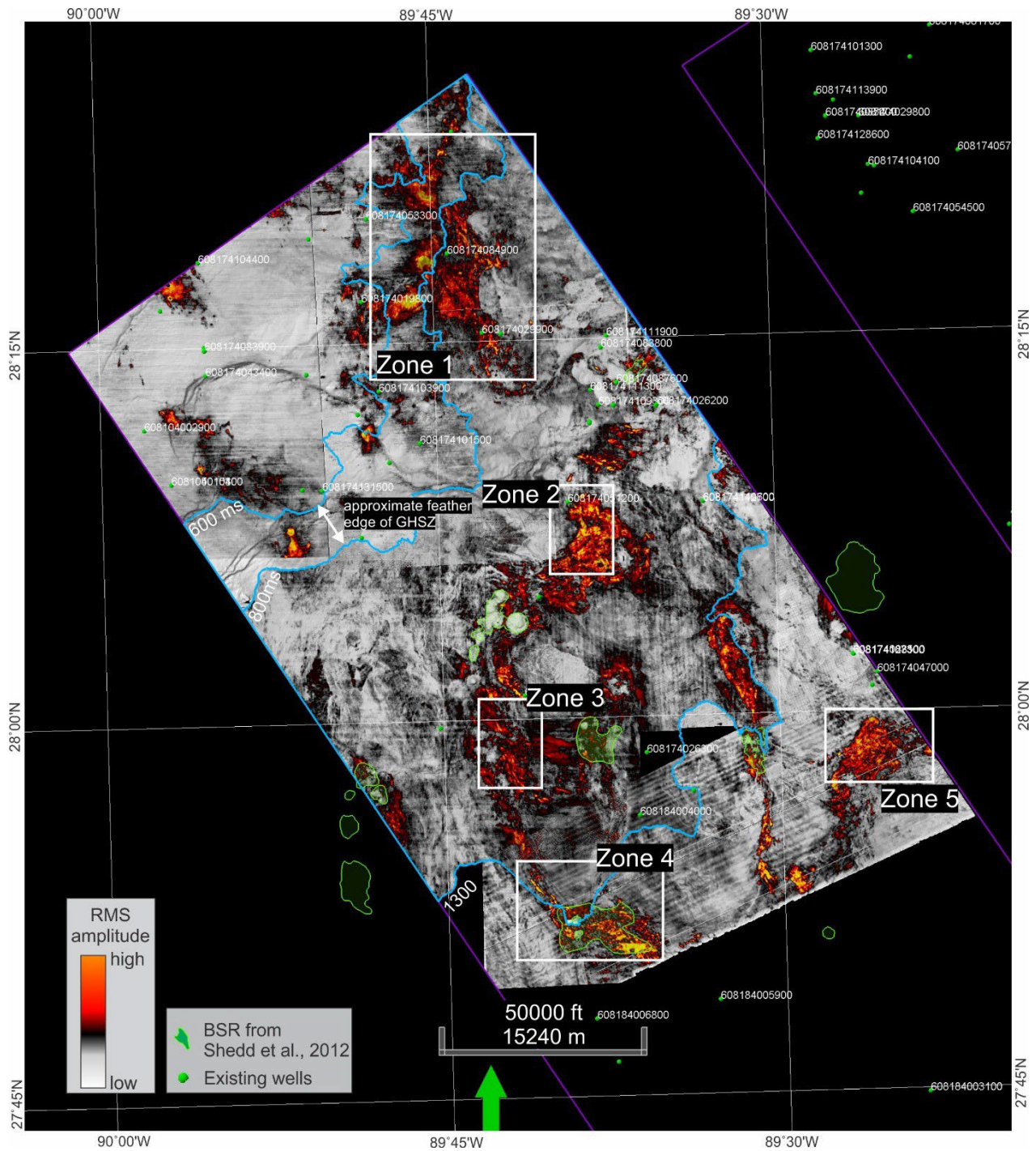


Figure 3. Major RMS amplitude map at the approximate level of the base of GHSZ within Project Area 3. Bathymetric contours 600, 800 and 1300 ms TWT dividing the area into three depth domains are shown with blue lines. The feather edge of GHSZ is located approximately between 600 and 800 ms TWT water depth (see Figure 9 for details). Labeled green dots show location of the wells drilled in the study area (labels are well APIs). Semi-transparent green areas show previously mapped BSR distribution (Shedd et al., 2012).

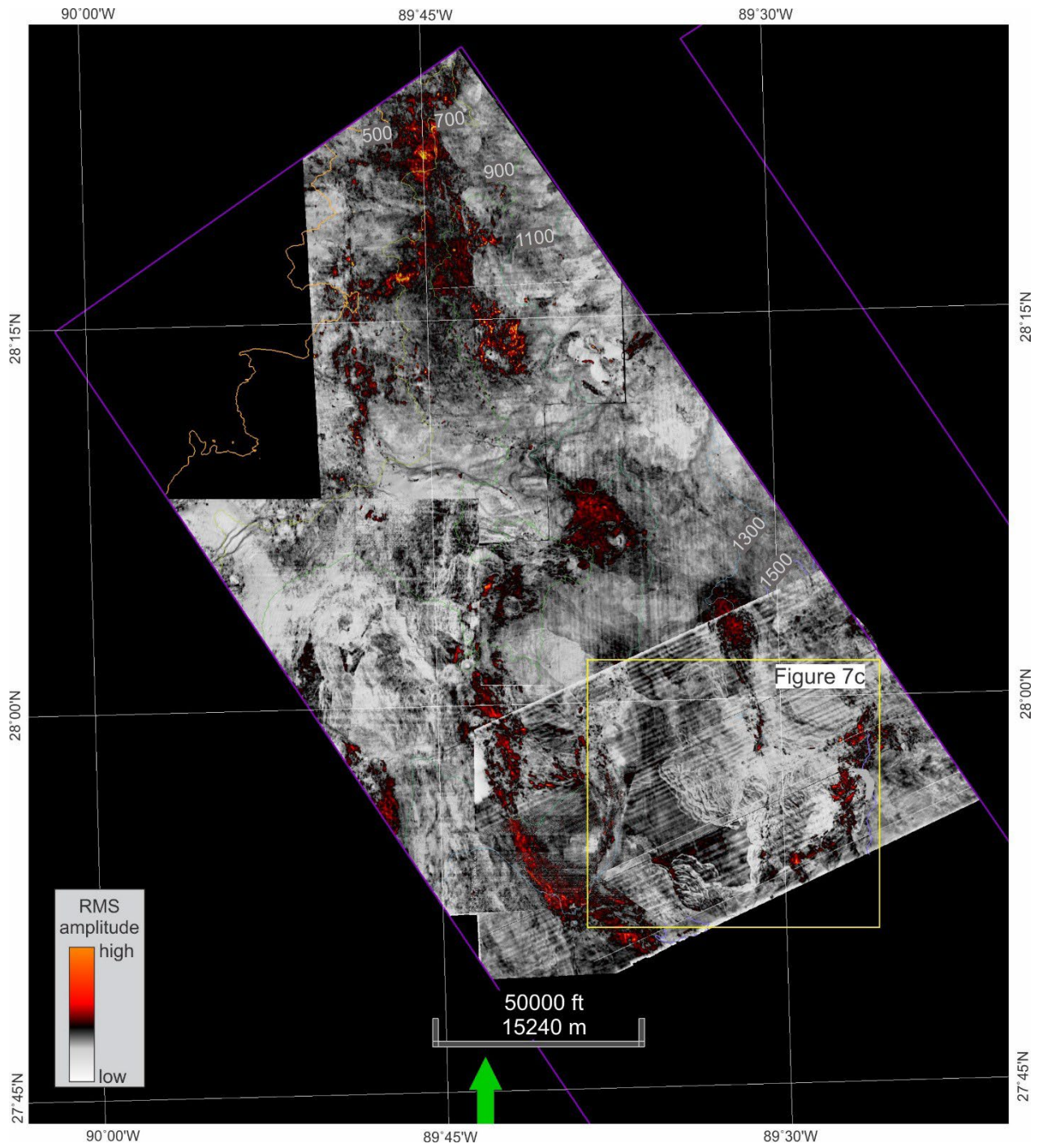


Figure 4. Secondary RMS amplitude map generated for mapping buried channels and landslides.



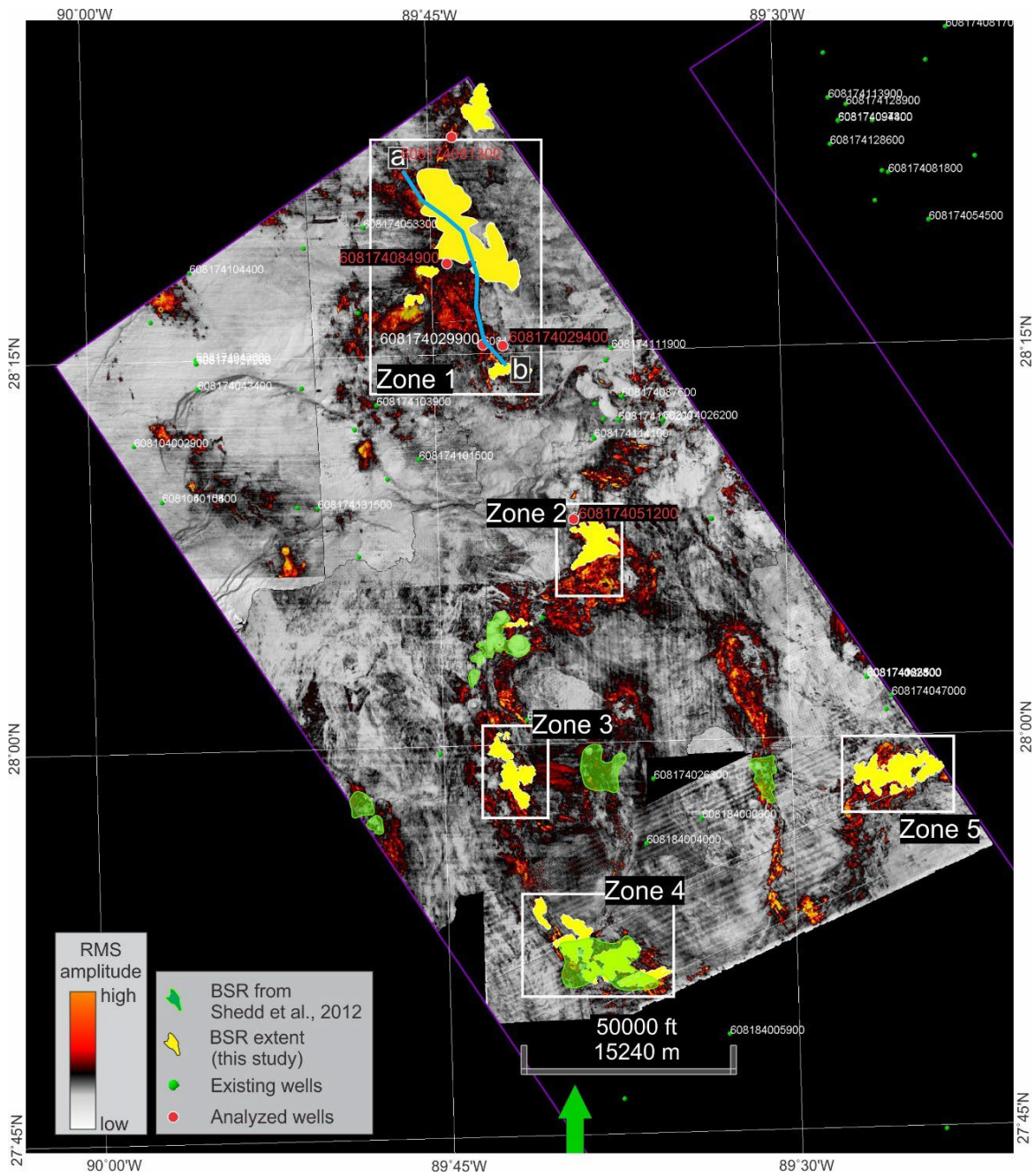


Figure 5. RMS amplitude map showing a minimum BSR extent within Project Area 3 (yellow areas). Semi-transparent green areas show previously mapped BSR distribution (Shedd et al., 2012). The minimum extent includes only the high-confidence areas, where we observe reflections sub-parallel to the seafloor. In many cases, open-source seismic data did not allow for resolving such reflections within high RMS zones (e.g. shown in Figure 10), however, BSRs can potentially be identified in a more recent data. Green dots show the surface well locations. Red circles show five wells selected for log data analyses. Five zones of interest are indicated with labeled white boxes.



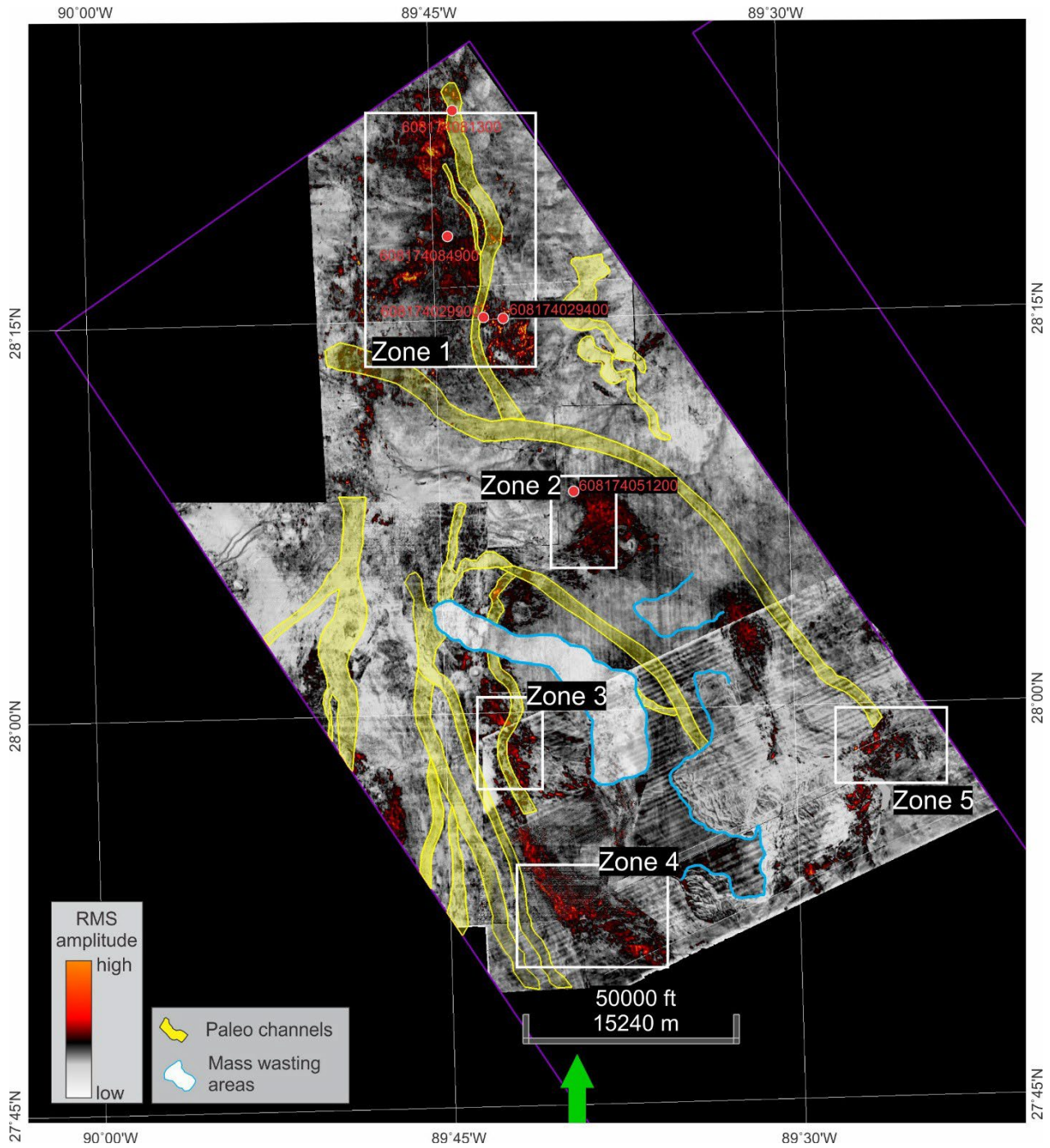


Figure 6. Secondary RMS map with interpreted buried channels (yellow) and landslide scars (blue).

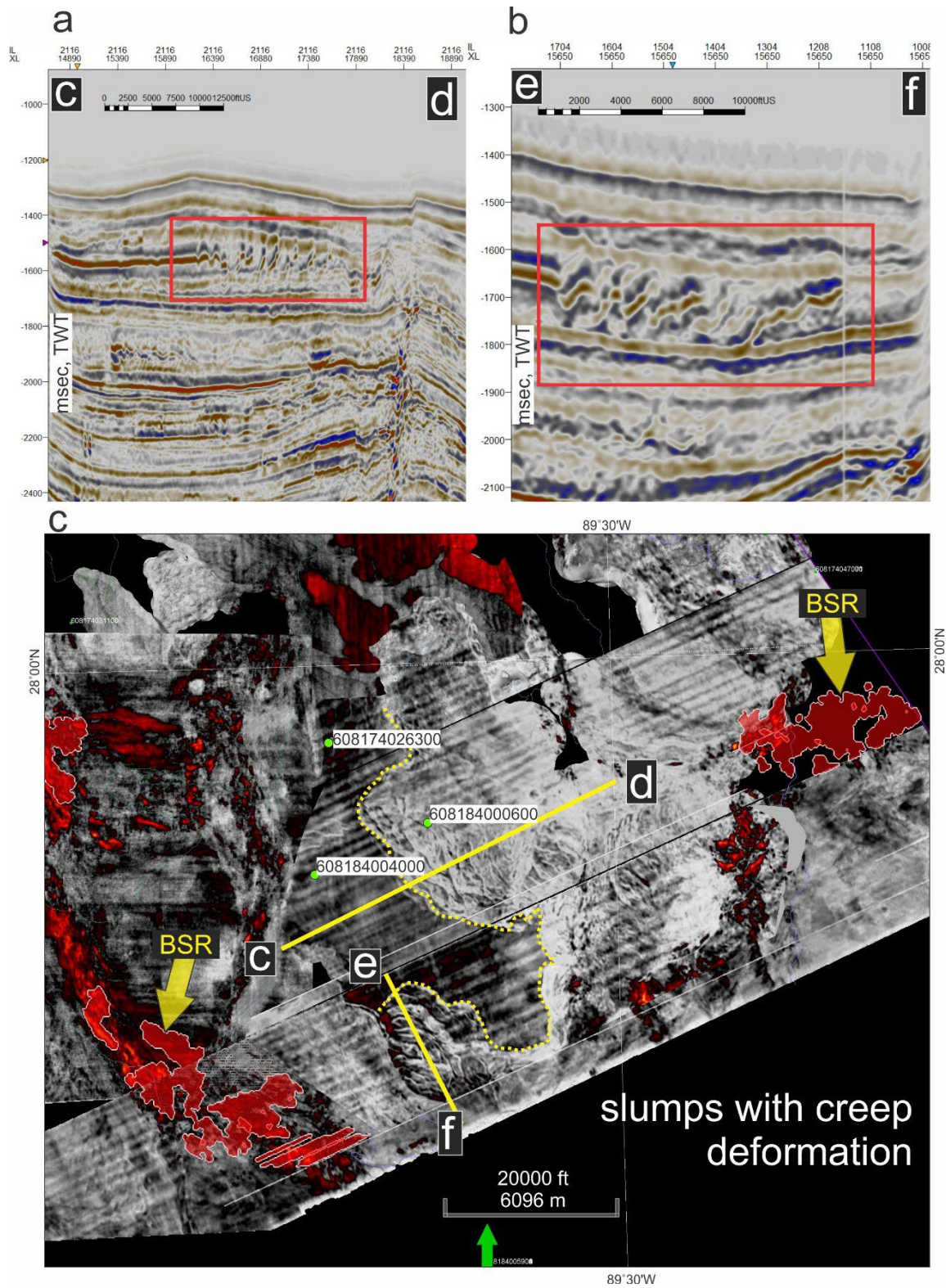


Figure 7. (a, b) Examples of slumps with creep deformation in the southern part of Project Area 3. c) Secondary RMS amplitude map showing distribution of mass wasting processes in the southern part of Project Area 3. Locations of lines c-d and e-f are indicated.

### **3. Results in Project Area 3**

#### **3.1 Paleo-channels and buried landslides**

Within Project Area 3 there are several large channels generally extending in northwest-southeast direction. Some segments of these channels were traced in the RMS maps, but in many places their location and extent were identified from manual mapping using principle of channel continuity (i.e. two channel segments were connected if they appeared to belong to the same channel system even if seismic data quality didn't allow for robust interpretation between them). We also suppose that there are systems of smaller connecting and meandering channels within Project Area 3 that are not resolvable in the open-source seismic data. Nevertheless, even the poor quality seismic data shows the existence of turbidite channel systems across Project Area 3, and BSRs mapped in Zones 1, 3, 4 and 5 may be associated with channel facies (Figure 5, 6). Additionally, as shown in Figure 2, the eastern portions of Project Area 3 are dominated by the Mississippi Canyon fill sediments limiting sedimentation mainly to slope processes at the canyon sidewall.

In the southern part of Project Area 3 several mass wasting events were identified (Figure 6, 7). Both, in map view and in cross sections we observed multiple paleo-escarpments and evidences of creep deformation indicative of slump processes on ancient slopes. Within the mass wasting areas no BSR or channel mapping was possible due to highly disturbed stratigraphy.

#### **3.2 Bottom-simulating reflections**

We identified five major zones of interest where BSRs were identified in the seismic data (Figures 5, 8, 9). BSRs in Zones 1, 2 and 4 are higher-confidence than in Zones 3 and 5, where seismic data quality doesn't allow for more detailed interpretation of such features as phase reversals. Similar to Project Area 2, BSRs are mainly attributed to anticlinal structures within salt roofs, as well as to the areas of active channel development (Figure 9).

The BSR in Zone 1 is the most remarkable. It extends along a western flank of a buried channel for more than 15 km and tappers out near the seafloor approximately at the feather edge of GHSZ (Figures 5, 9, 10, 11). To our knowledge, it is a first example of a BSR documented at the feather edge of GHSZ in the Gulf of Mexico, and one of the few examples known worldwide. Please see Zone 1 discussion further in the report for more details.

Structure maps were only generated for Zones 2 and 4 because in other Zones there were no coherent seismic reflections at or above the BSR level in the available seismic data.



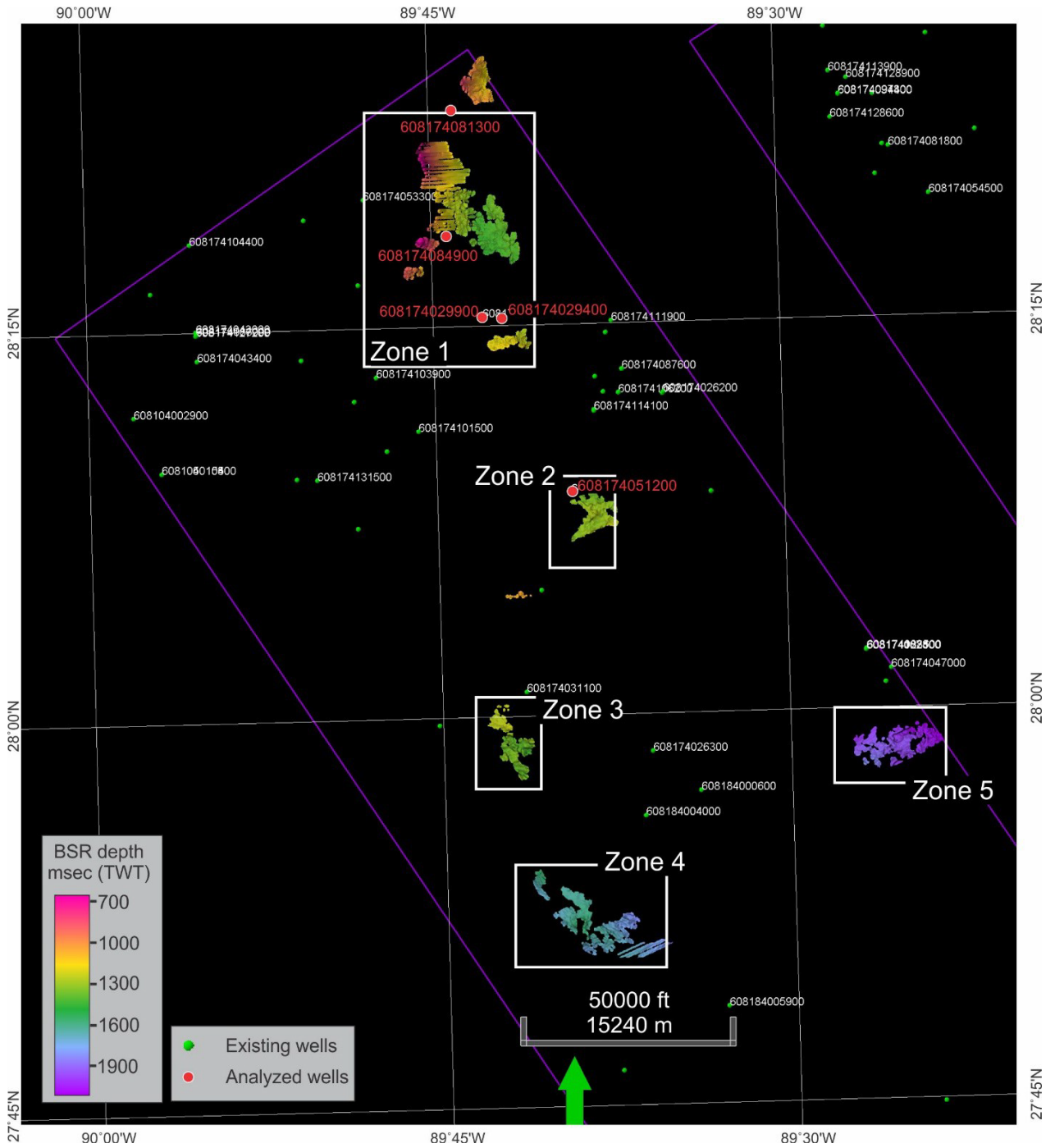


Figure 8. Depth of manually and semi-automatically mapped BSR. Wells and zones of interest are indicated and labeled.

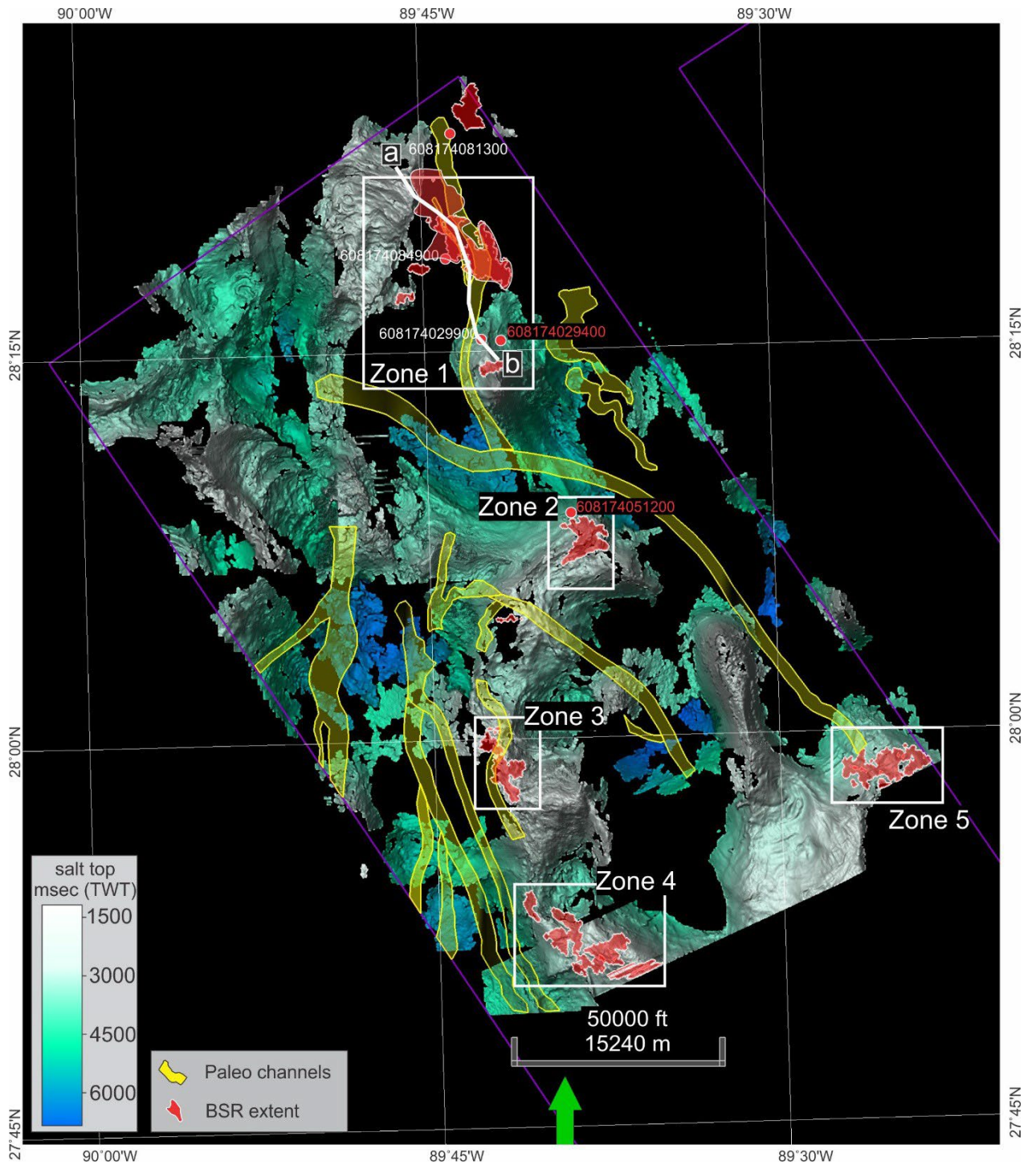


Figure 9. Top of salt depth (blue-green white), paleo-channels and BSR distribution interpreted from RMS amplitude maps.

## 4. Results in Zones 1-5

### 4.1 Zone 1

The highest RMS amplitudes at the inferred base of GHSZ are concentrated along the channel (Figures 5, 9, 10) at ~100-350 ms TWT below the seafloor. These high amplitude reflections form an extensive BSR observed in seismic cross sections (Figure 10a, b). In the northern part of Zone 1, subseafloor depth of the BSR shoals, and in ~650-800 ms water depth (487-600 mbsl) it merges with the seafloor reflection. Based on the average annual bottom water temperatures, this water depth interval agrees with the depth of the feather edge of GHSZ in the Gulf of Mexico (Figure 10a, inset). Therefore, high RMS amplitude values indicate gas concentrated at the base of GHSZ in channel levee and overbank sediments. A cross plot of the RMS amplitude values against depth (msec TWT) shows that the highest RMS amplitudes occur around the feather edge of GHSZ (Figure 10c), which is supported by a BSR tapering out at the seafloor in the northern part of Zone 1.

Well log data from three wells drilled within the high amplitude anomalies were ordered from the Bureau of Safety and Environmental Enforcement for analyses (API: 608174084900, 608174029900, 608174029400). Unfortunately, only well 608174029400 includes log data from the shallow interval. In wells 608174029900 and 608174029400 logging started at 9400 and 4000 ft MD respectively, which is significantly below the base of GHSZ at these locations (~3200 fbsl) (Figure 11b). In well 608174084900 we do observe a slight increase in resistivity from 1 to 2.4  $\Omega$ m between 2700 and 2900 ft MD. This interval agrees with the approximate base of GHSZ based on a reasonable geothermal gradient 30 °C/km and average annual bottom water temperature ~5.5 °C at 2150 fbsl (top hole water depth). In the absence of digital well log data, we used a 1550 m/s acoustic velocity for time-depth conversion. Seismic data at the base of GHSZ around well 608174084900 show chaotic clusters of high-amplitude reflections without a clear BSR, therefore it is not evident whether the elevated resistivity is related to gas hydrate or free gas below the base of GHSZ or both.



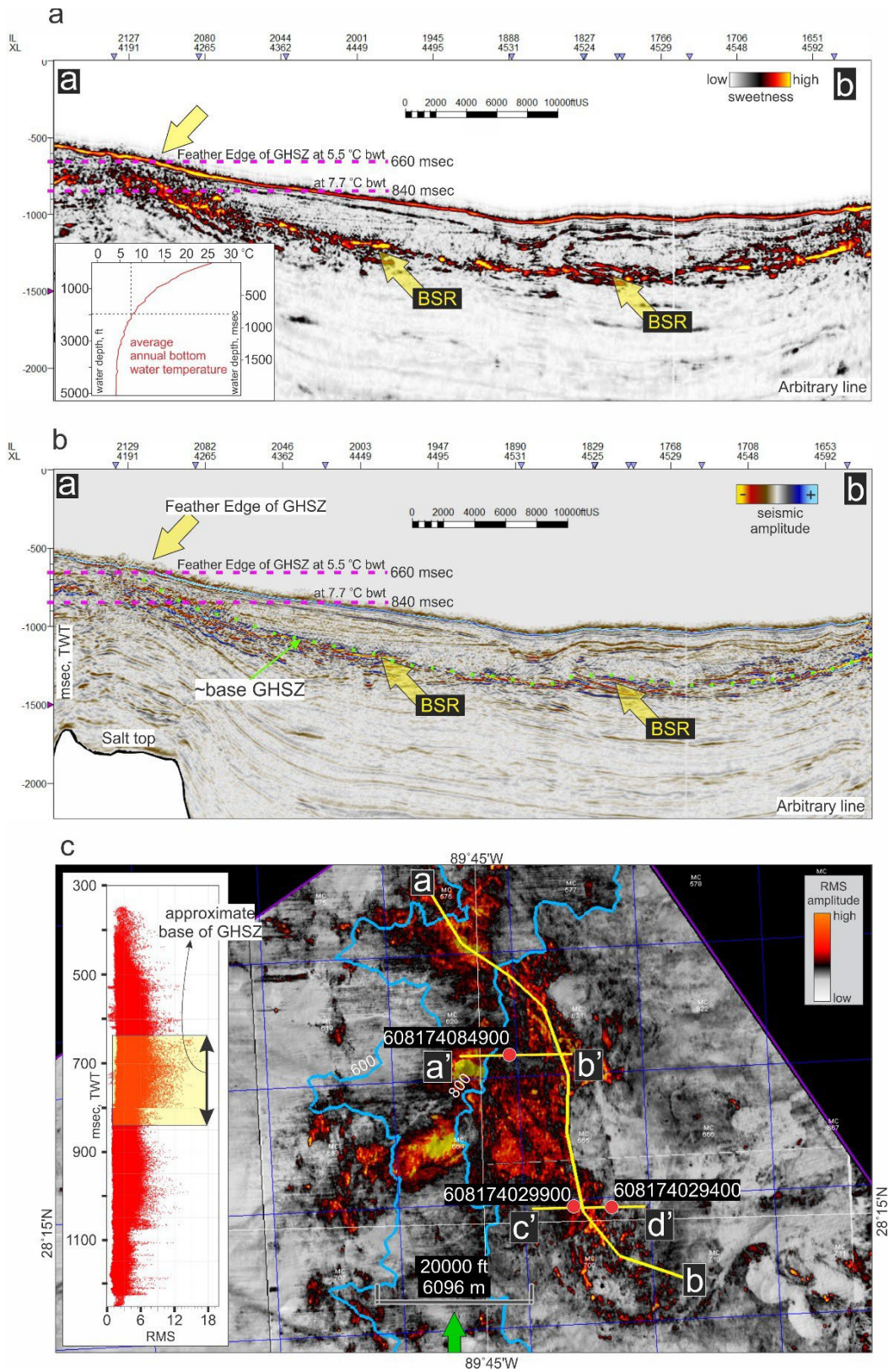


Figure 10. Sweetness attribute (a) and seismic amplitude (b) cross sections along an arbitrary line a-b following the strong RMS amplitude anomaly in Zone 1. Location of line a-b is indicated in Figure 10c. c) RMS amplitude map of Zone 1 with location of seismic cross sections in Figure 10a, b and Figure 11 and three wells. Blue lines are 600 and 800 ms TWT bathymetric contours (450 and 600 mbsl respectively). License blocks are shown in purple.



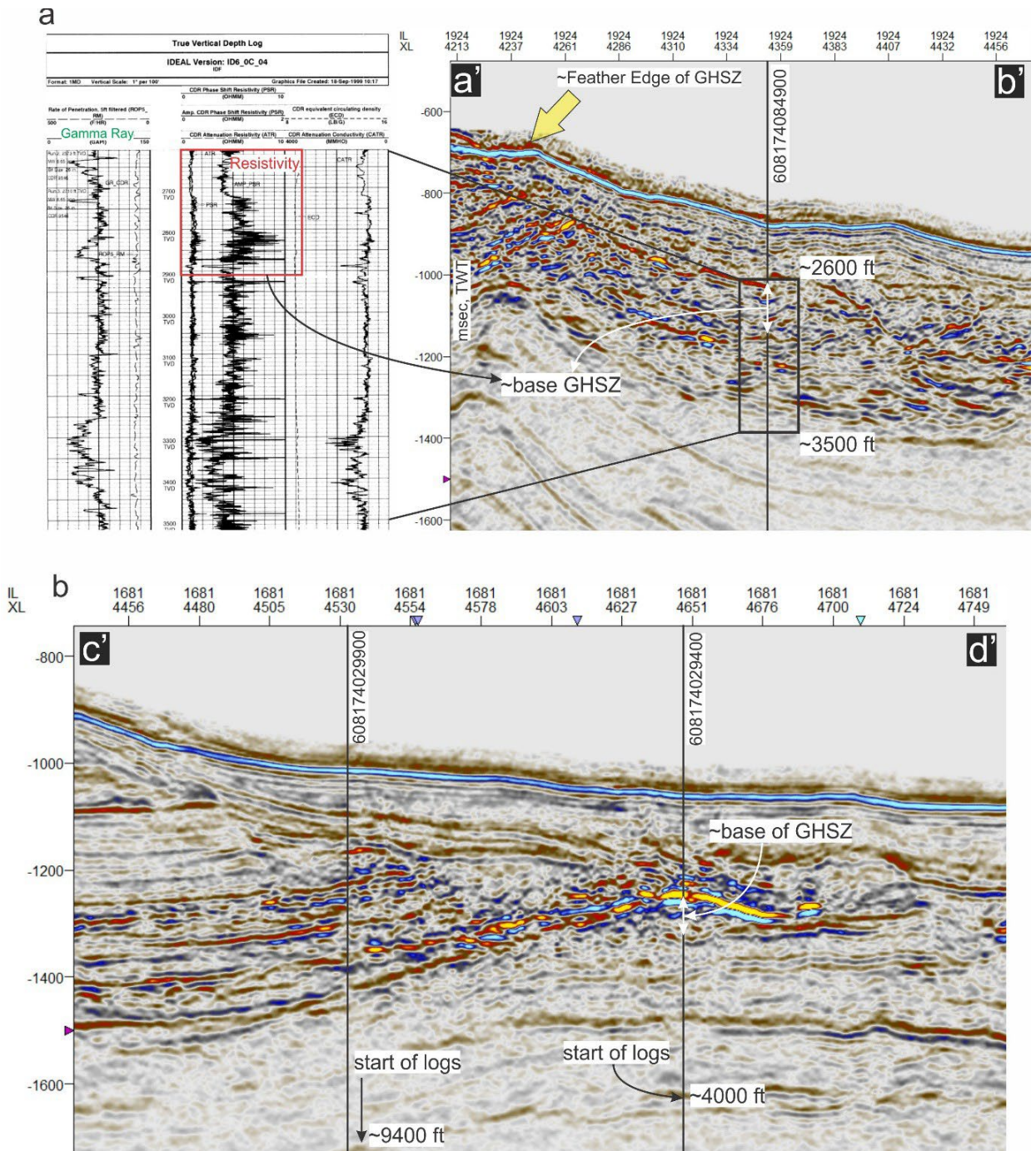


Figure 11. a) Gamma ray and resistivity logs in well 608174084900 and approximate depth of selected log interval 2600-3500 ft MD in the seismic cross section a'-b' (location is shown in Figure 10c). b) location of wells 60817402900 and 608174029400 on the seismic cross section c'-d' showing that log data start significantly below the base of GHSZ (location of c'-d' is indicated in Figure 9c).

## 4.2 Zone 2

RMS amplitudes in Zone 2 show anomalously high values above a salt uplift (Figures 9, 12b, 12c, 14). The BSR in Zone 2 can be classified as discontinuous on some lines (e.g. Figure 12a), continuous (Figure 12d) and clustered (Figure 14c) depending on the direction of cross sections. A phase reversal is observed in the northwestern part of the amplitude anomaly (line g-h in Figure 12a) with a strong trough-leading reflection below the base of GHSZ changing to a peak-leading reflection above.

The most proximal well to the BSR in Zone 2 is well 608174051200. Increased resistivity up to 2-3  $\Omega\text{m}$  is observed at the approximate base of GHSZ in the interval 3000-3600 ft MD (Figure 13) likely indicating low-concentration gas hydrate. This interval is also characterized by lower gamma ray values, however there is no evidence for channelizing and in the seismic data around well 608174051200. On the well log data, the resistivity peaks at 2-3  $\Omega\text{m}$  do not consistently correlate with gamma ray lows, suggesting the hydrate accumulation may be in marine muds.

Importantly, gas hydrates have been previously sampled in Zone 2 in Block MC 798 from a seafloor mound (Figure 12b, c, Figure 14c) (Geresi et al., 2002; Neurauter & Bryant, 1989). This seafloor mound is located over the area of anomalously high seismic amplitudes and close to where strong peak-leading amplitudes were mapped above the base of GHSZ (Figure 12b, c). Figure 14c shows that the gas hydrate bearing mound sits on top of a deep-rooted fault, which runs through the clustered BSR in Zone 2 and extends down to  $\sim 1800$  ms TWT. This is an important observation indicating active upward fluid flow through the GHSZ from its base marked by BSR towards the seafloor.

## 4.3 Zones 3-5

Zones 3, 4 and 5 in Project Area 3 are located above salt domes where high-amplitude clustered reflections were observed in the seismic data (Figures 15, 16, 17). To provide a higher-confidence interpretation within these zones a better resolution seismic data and/or well data are required. Previously, similar multiple high-amplitude reflections within anticlinal folds at the base of GHSZ were interpreted as clustered BSRs potentially indicating entrapment of gas within coarse-grained turbidites (Portnov et al., 2019). Such structural settings involving faulting and folding within salt roofs (also observed in Zones 3-5, see Figures 15, 16, 17) are among the most common for BSR occurrence in the Gulf of Mexico. Therefore, we preliminary interpret clustered reflections in Zones 3-5 as low-confidence gas/gas hydrate accumulations that require further analyses.



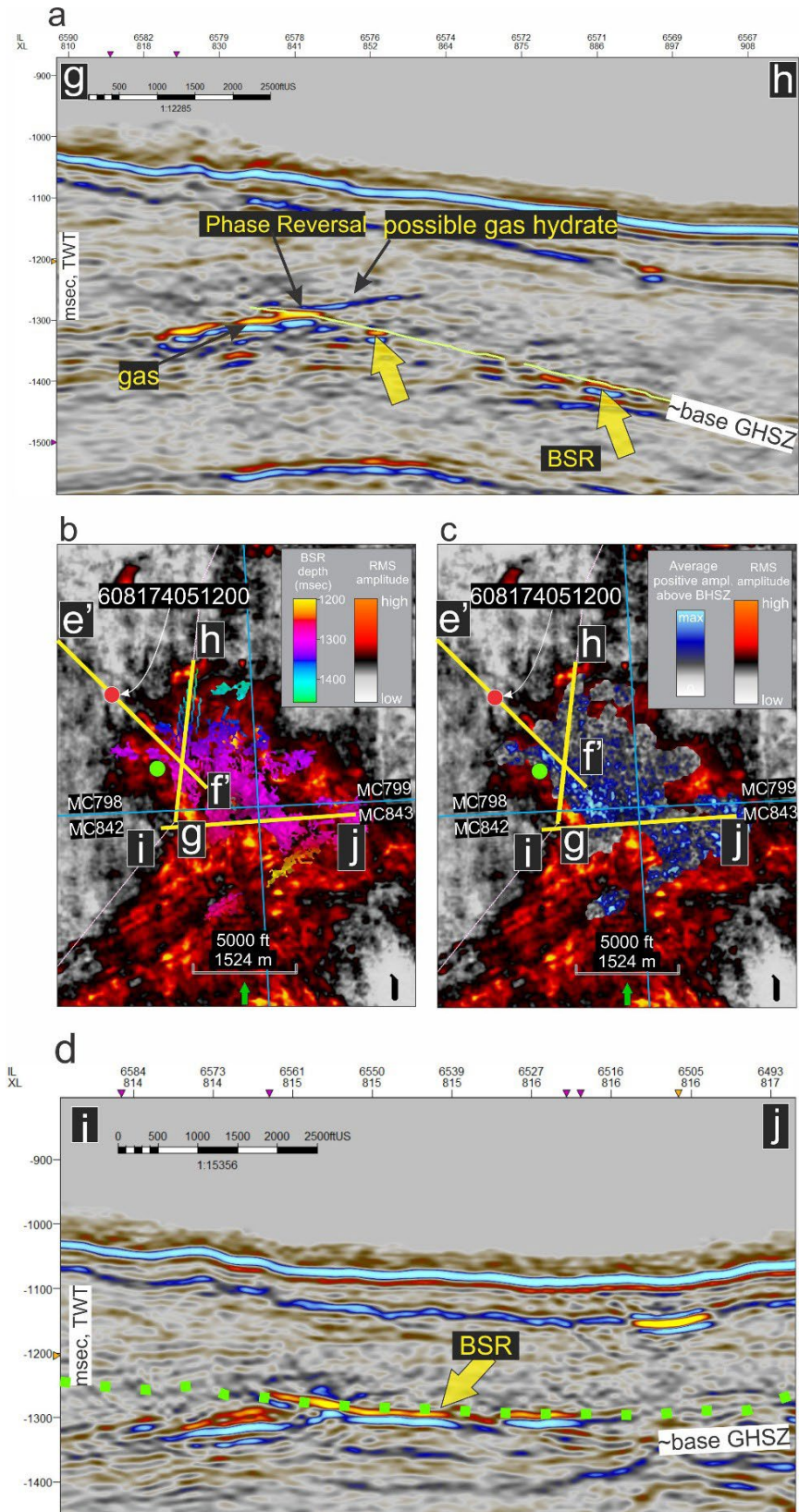


Figure 12. a) Seismic cross section g-h showing discontinuous BSR and amplitude phase reversal b) RMS amplitude and BSR depth map in Zone 2. A red circle shows top hole location of well 608174051200, and a green circle shows seafloor location of gas hydrate bearing mound c) RMS amplitude map and average positive amplitudes above the base of GHSZ in Zone 2, d) Seismic cross section i-j showing continuous BSR and possible gas accumulation below.

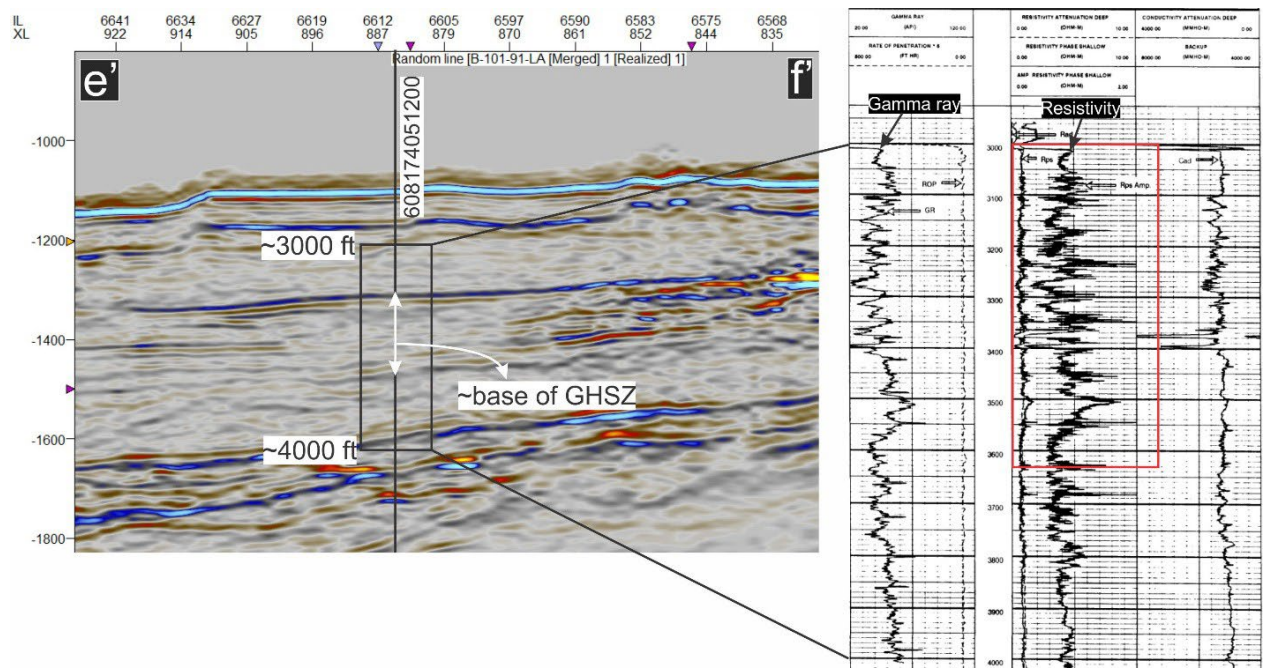


Figure 13. Top hole location of well 608174051200 and gamma ray and resistivity logs in this well. Logs show elevated resistivity at the approximate base of GHSZ. Position of the seismic cross section is indicated in Figure 12a.



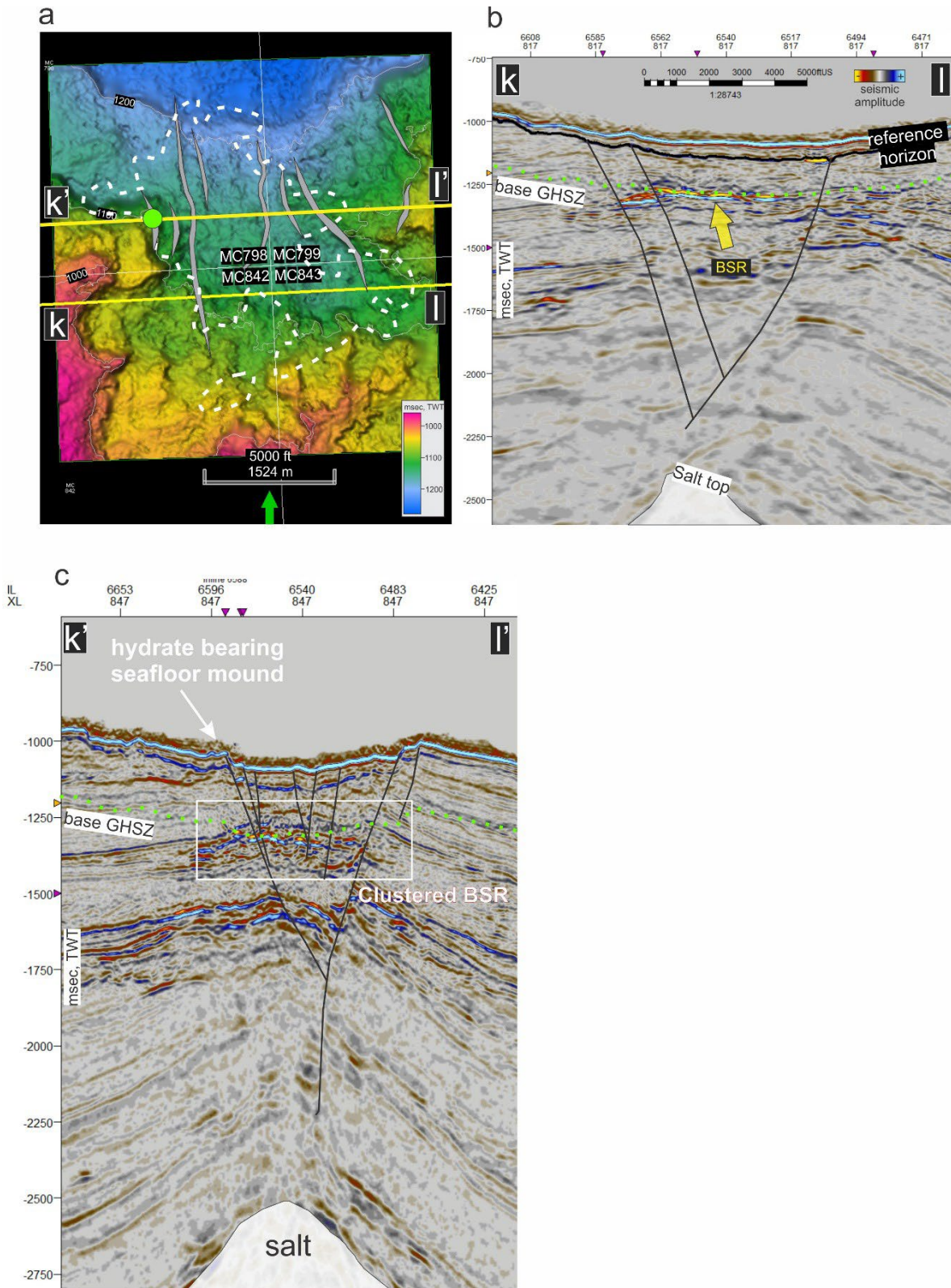


Figure 14. a) Time structure map along the closest overlying coherent horizon in Zone 2. Green circle shows seafloor location of the gas hydrate bearing mound. White dashed line shows approximate BSR limit b) seismic cross section k-l (position is indicated in Figure 14a) showing the top of salt below the BSR in Zone 2 c) Seismic cross section k'-l' (location in Figure 14a) showing position of the seafloor hydrate bearing mound above a clustered BSR in Zone 2.



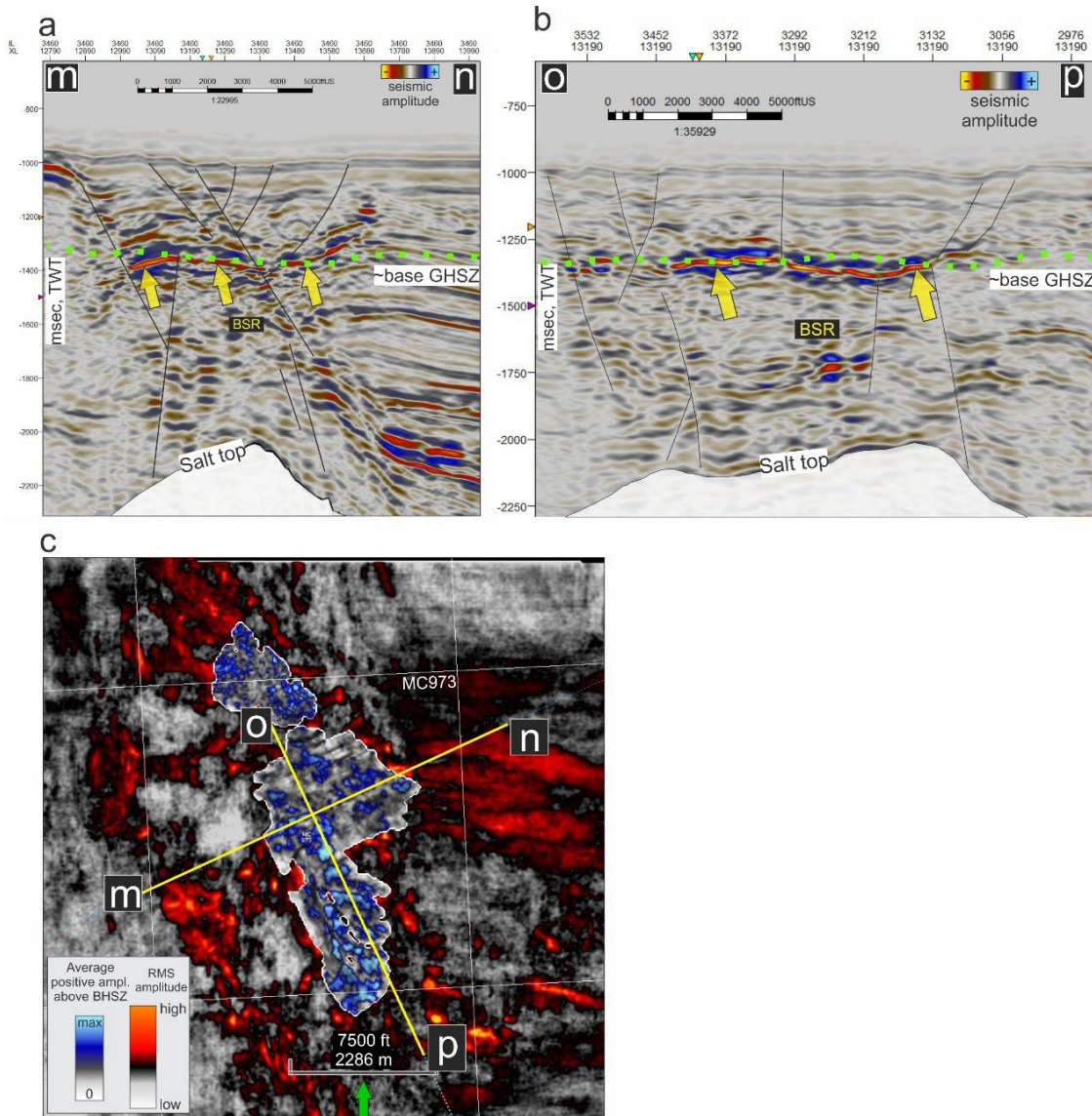


Figure 15. a) Cross section m-n showing possible clustered BSR in a salt roof in Zone 3, b) Cross section o-p showing possible clustered BSR in a salt roof in Zone 3, c) RMS amplitude and average positive amplitudes above the base of GHSZ in Zone 3. Location of seismic cross lines o-p and m-n are indicated.

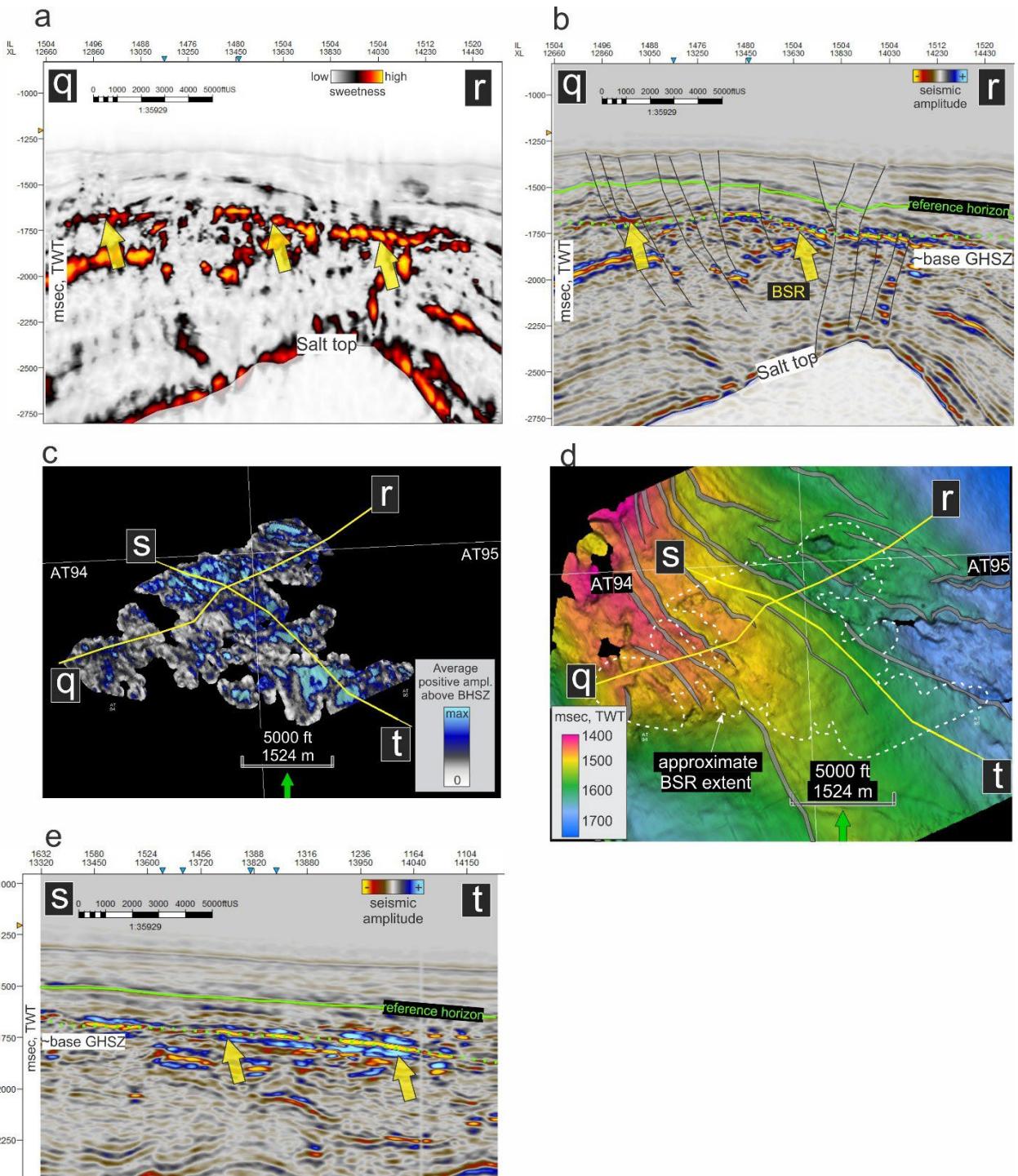


Figure 16. Possible BSR in Zone 4 illustrated along arbitrary line q-r in sweetness attribute cross section (a) and seismic amplitudes cross section (b), c) Average positive amplitudes above the base of GHSZ in Zone 4, d) Time structure map along a reference horizon indicated in Figure 16b. Dashed white line shows approximate BSR limits. Locations of arbitrary lines q-r and s-t are shown in Figures 16c and d, e) Seismic amplitude cross section s-t showing possible BSR in Zone 4.



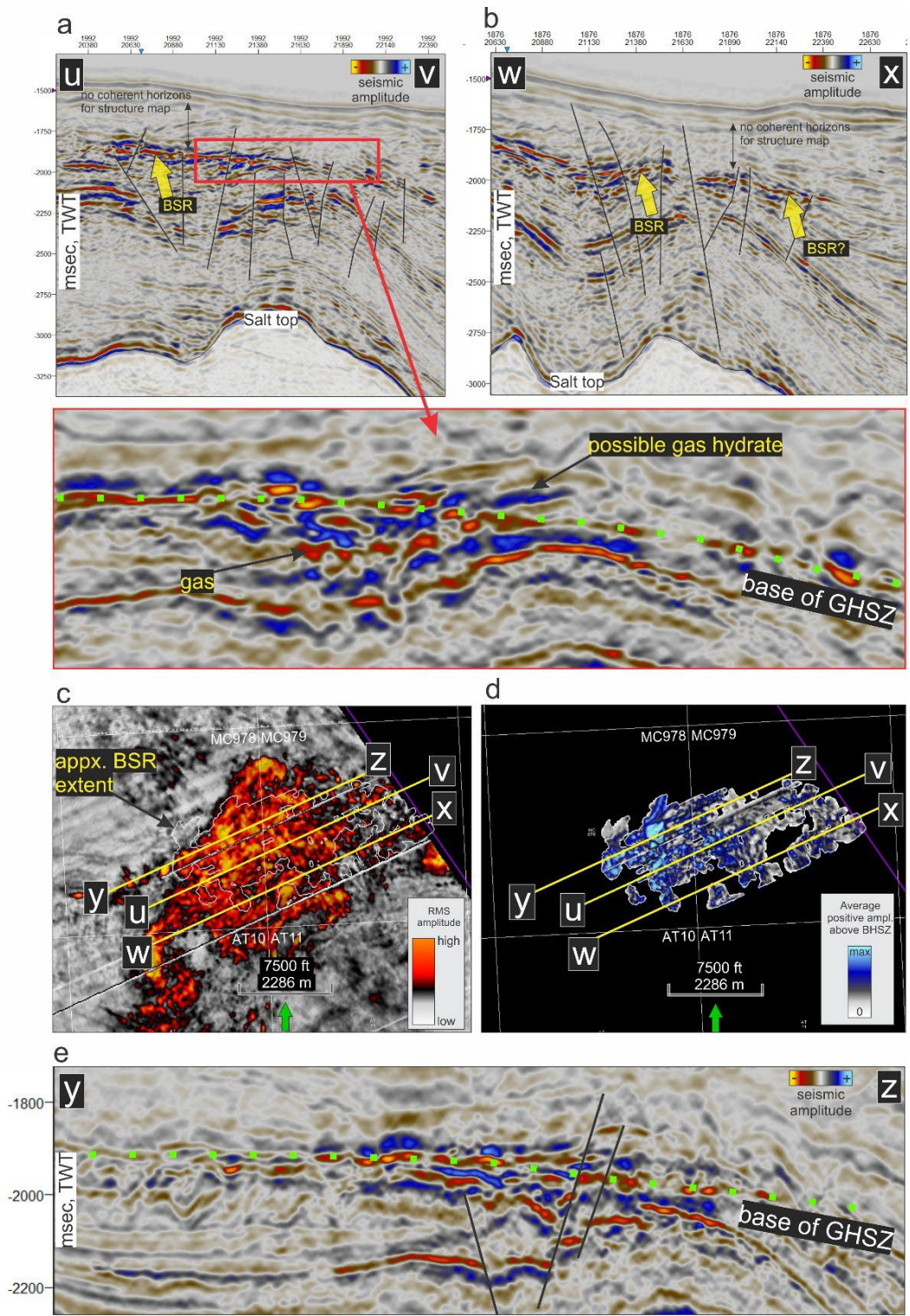


Figure 17. Seismic amplitude cross sections u-v (a) and w-x (b) showing a possible clustered BSR in Zone 5, b) RMS amplitude map in Zone 5 with approximate BSR limits indicated with white line, c) Map of average positive amplitudes above the base of GHSZ, d) Another seismic amplitude cross section y-z at the base of GHSZ. Locations of lines u-v, w-x and y-z are indicated in Figure 17c and d.



## 5. Gas resource estimates

We used the same minimum and maximum porosity values (30% and 40% respectively) as in the Project Areas 1 and 2. We applied minimum and maximum sand thicknesses of 10 and 50 m. Similar to the Project Areas 1 and 2 we used minimum and maximum gas hydrate saturations within these sand units of 50 and 90%.

The total area of BSRs in Zones 2-5 is ~31 km<sup>2</sup>, which results in minimum and maximum gas resource estimates of 7.75 and 93 BCM respectively at STP (standard temperature and pressure) conditions (which uses a gas hydrate to gas conversion factor = 164). Given that 50 and 90% gas hydrate saturation should be confined to the areas with high-amplitude peak-leading amplitudes (~5 km<sup>2</sup>) the high-saturation gas hydrates in Project Area 3 may contain between 1.24 and 15 BCM of gas.

## 6. Conclusions

Potential gas hydrate occurrences in Project Area 3 are associated with several buried channel-levee systems that deposited sand-bearing units at the approximate modern base of BHSZ. In the central part of Project Area 3, underlying salt bodies create anticlinal structures favorable for entrapment of gas at the BHSZ and formation of clustered BSRs that are good indicators of high-saturation gas hydrate reservoirs in turbidites (Portnov et al., 2019). The first priority are Zones 1 and 2. Zone 1 potentially includes one of the shallowest gas hydrate occurrences known in the Gulf of Mexico, located at the feather edge of the GHSZ. This region may be selected for future investigations because processes of gas hydrate formation and recycling at the feather edge are important particularly for slope stability and ocean acidification. Zone 2 shows an amplitude phase reversal that is evident even in the poor-quality open-source data. A clear BSR, elevated resistivity in low gamma ray units and previously documented gas hydrate bearing mound at the seafloor increase the likelihood of gas hydrate accumulations in Zone 2.

## 7. References

- Geresi, E., Lutken, C., Mcgee, T., & Lowrie, A. (2002). *Complex Geology and Gas Hydrate Dynamics Characterize Mississippi Canyon Block 798 on the Upper Continental Slope of the Northern Gulf of Mexico* (Vol. 52). GCAGS Transactions.
- Goodwin, R. H., & Prior, D. B. (1989). Geometry and depositional sequences of the Mississippi Canyon, Gulf of Mexico. *Journal of Sedimentary Petrology*, 59(2), 318–329. <https://doi.org/10.1306/212F8F85-2B24-11D7-8648000102C1865D>
- Neurauter, T. W., & Bryant, W. R. (1989). *GAS HYDRATES AND THEIR ASSOCIATION WITH MUD DIAPIR/MUD VOLCANOES ON THE LOUISIANA CONTINENTAL SLOPE*.
- Portnov, A., Cook, A. E., Sawyer, D. E., Yang, C., Hillman, J. I. T., & Waite, W. F. (2019). Clustered BSRs: evidence for gas hydrate-bearing turbidite complexes in folded regions, example from the Perdido Fold Belt, northern Gulf of Mexico. *Earth and Planetary Science Letters*.
- Shedd, W., Boswell, R., Frye, M., Godfriaux, P., & Kramer, K. (2012). Occurrence and nature of “bottom simulating reflectors” in the northern Gulf of Mexico. *Marine and Petroleum Geology*, 34(1), 31–40. <https://doi.org/10.1016/j.marpetgeo.2011.08.005>